Drug Design, Development and Therapy Dovepress

Open Access Full Text Article ORIGINAL RESEARCH

OmpH is Involved in the Decrease of *Acinetobacter baumannii* Biofilm by the Antimicrobial Peptide Cec4

Zhilang Qiu[1,2,*], Jun Ran[1,2,*], Yifan Yang[1,2,*], Yue Wang[1,2], Yang Zeng[1,2], Yinhui Jiang[1], Zuquan Hu[1], Zhu Zeng[1], Jian Peng[1,2]

[1]Key Laboratory of Infectious Immune and Antibody Engineering of Guizhou Province, Cellular Immunotherapy Engineering Research Center of Guizhou Province, School of Biology and Engineering/School of Basic Medical Sciences, Guizhou Medical University, Guiyang, Guizhou, 550025, People's Republic of China; [2]The Engineering Research Center of Health Medicine Biotechnology of Institution of Higher Education of Guizhou Province, Guizhou Medical University, Guiyang, Guizhou, 550025, People's Republic of China

*These authors contributed equally to this work

Correspondence: Jian Peng; Zhu Zeng, Email jianpeng@gmc.edu.cn; zengzhu@gmc.edu.cn

Purpose: The emergence of carbapenem-resistant *Acinetobacter baumannii* (CRAB) poses great difficulties in clinical treatment, and has been listed by the World Health Organization as a class of pathogens in urgent need of new antibiotic development. In our previous report, the novel antimicrobial peptide Cec4 showed great potential in decreasing the clinical CRAB biofilm, but its mechanism of action is still illusive. Therefore, in order to evaluate the clinical therapeutic potential of Cec4, it is necessary to explore the mechanism of how Cec4 decreases mature biofilms.

Methods: Key genes involved in the removal of CRAB biofilms by Cec4 were analyzed using transcriptomics. Based on the results of the bioinformatics analysis, the CRISPR-Cas9 method was used to construct the deletion strain of the key gene. The pYMAb2 plasmid was used for the complementation strain construction. Finally, the roles of key genes in biofilm removal by Cec4 were determined by crystal violet staining, podocyte staining, laser confocal imaging, and MBC and $MBEC_{50}$.

Results: Combined with transcriptome analysis, we hypothesized that *OmpH* is a key gene involved in the removal of CRAB biofilms by Cec4. Deletion of the *OmpH* gene did not affect *A. baumannii* growth, but decreased *A. baumannii* capsule thickness, increasing biofilm production, and made biofilm-state *A. baumannii* more sensitive to Cec4.

Conclusion: Cec4 decreases biofilms formed by CRAB targeting *OmpH*. Deletion of the *OmpH* gene results in an increase in biofilms and greater sensitivity to Cec4, which enhances the removal of *A. baumannii* biofilms by Cec4.

Keywords: *Acinetobacter baumannii*, antibiofilm mechanism, antimicrobial peptide, *OmpH*

Introduction

Acinetobacter baumannii, a gram-negative pathogen commonly found in intensive care units (ICUs) and operating rooms, is an important opportunistic pathogen in healthcare facilities throughout the world.[1] They tend to acquire multidrug resistance and even pan-resistant phenotypes at a previously unforeseen rate.[2] Multidrug-resistant *A. baumannii* is a concern, because it is responsible for approximately 60% of hospital-acquired infections. It can cause various infections, including ventilator-associated pneumonia, bloodstream and skin and tissue infections, in both healthy and immunocompromised individuals.[3] Unfortunately, the development of antibiotics against gram-negative bacteria has remained stagnant, owing to their diverse resistance mechanisms.[4]

A biofilm is an extracellular matrix of polysaccharides, extracellular DNA, and secreted proteins produced by bacteria, which come together to form a bacterial community.[5] Biofilms are the leading cause of antibiotic resistance in *A. baumannii*, and most infections are caused by biofilms. The formation of biofilm from adhesion to mature diffusion involves gene regulation of various systems of *A. baumannii*. For example, *Csu* operon of fimbrial system responsible for adhesion, while Csu fimbrial is regulated by genes related to quorum sensing system and the two-component systems *BfmS/R* and *GacSA*. As well as genes such as the outer membrane protein family (OMP), which is responsible

Received: 27 July 2024
Accepted: 26 November 2024
Published: 7 December 2024

for the initiation of biofilm formation, and phosphoglucose mutase *PGM*, which makes up the biofilm matrix.[6] These genes are closely related to the biofilm formation process of *A. baumannii*. Biofilms render bacteria highly resistant to antibiotic treatment, resulting in a mortality rate of 40–60%.[7] The *A. baumannii* ST1894 isolate showed a 2048-fold increase in resistance to imipenem and a 32-fold increase in resistance to fucoxanthin in the biofilm state.[8] The structure of biofilm antibiotics killed bacterial biofilm formation. Infections resulting from biofilms can persist for weeks or months and become antibiotic-resistant over time. Moreover, these infections can spread to other organs, resulting in prolonged clinical infections.[9,10] It is evident that *A. baumannii* in the biofilm state poses a greater threat than *A. baumannii* in the planktonic state.[9] Therefore, treatment of *A. baumannii* in the biofilm state is crucial for clinical treatment.

Antimicrobial peptides (AMPs) are crucial elements of the innate immunity in humans and other organisms. Currently, they are the major focus of antimicrobial research and development.[11] AMPs are short-chain polypeptides that typically contain fewer than 50 amino acids, and are amphiphilic.[12] AMPs generate a net positive charge on the peptide chains. Consequently, they easily bind to the negatively charged bacterial membranes, inhibiting bacterial growth, and initiating bactericidal action.[13] Previous studies have demonstrated that AMPs hinder or eliminate bacterial biofilms via three primary mechanisms.[14] These mechanisms include disrupting cellular signaling systems,[15] inhibiting the alarm system to prevent bacterial over reactivity, suppressing RNA synthesis,[16] and downregulating the expression of binding protein transporter genes responsible for biofilm formation.[17] However, the process by which AMPs eliminate biofilms is complex and necessitates additional investigation.[18]

The AMP cecropin-4 (Cec4) has good antimicrobial activity against gram-negative bacteria, particularly *A. baumannii*.[19,20] Preliminary studies have shown that Cec4 effectively removes carbapenem-resistant *A. baumannii* biofilm.[21] However, the targets of Cec4 and the mechanism by which it removes *A. baumannii* biofilm remain unclear. Based on our previous study, we performed transcriptome and proteome analyses of Cec4 to clear carbapenem-resistant *A. baumannii* biofilms using high-throughput sequencing and tandem mass spectrometry. Based on omics analysis, we knocked out genes to investigate the regulatory mechanisms and potential targets of Cec4 in the process of *A. baumannii* biofilm clearance.

Materials and Methods

Strain Culture Conditions and Cec4

A. baumannii ATCC 17978 was maintained at the School of Biology and Engineering, Guizhou Medical University. Cec4 (GWLKKKIGKKKIERVGQNTRDATIQAIGVAQQQAANVAATLKGK) was synthesized with a purity of > 97% by high-performance liquid chromatography (HPLC) using solid-phase chemical synthesis at Gill Biochemicals (Shanghai) Co. Ltd.

The experimental bacteria were stored at −80 °C. Glycerol stocks were removed from storage and dipped into the inoculating ring for plate delineation. After overnight incubation at 37°C, single colonies were picked and incubated in 5 mL of Luria-Bertani (LB) liquid medium at 37°C Shock incubator with 220 rpm until the logarithmic growth period for the following phenotyping experiments.

Transcriptome Data Analysis

Bipartite sequencing data from the Sequence Read Archive (SRA) (PRJNA607078) were downloaded from the National Center for Biotechnology Information (NCBI) and subjected to quality control filtering using fastp software (https://github.com/OpenGene/fastp) to remove unknown bases and fragments with poor sequencing quality, resulting in clean read files. Transcriptome data were analyzed using the R statistical program (https://cran.r-project.org/) and the Bioconductor project (https://www.bioconductor.org/) provided by the software packages using the *A. baumannii* ATCC 19606 reference genome.

Bioinformatics Analysis of *OmpH*

Since there are few reports on OmpH, we conducted biological information prediction for this gene and submitted the protein sequence of this gene to SignalP (version 5.0), TMHMM, and SMART for signal peptide, transmembrane structure, and domain analyses, respectively. Hydrophilicity was predicted using the ProtScale. OmpH and Cec4 were modeled using

Discovery Studio 2019 (DS2019) and AlphaFold2.[22] DS2019 was used to dock OmpH with the Cec4. The results were visualized and analyzed using DS2019 software.

In addition, we searched for the OmpH of *Escherichia coli*,[23] *Bdellovibrio bacteriovorus*,[24] *Flavobacterium psychrophilum*,[25] *Pasteurella multocida*,[26] *Klebsiella* sp.[27] We conducted OmpH similarity detection using NCBI's Basic Local Alignment Search Tool and selected 4 proteins with 100% query coverage and identity. Subsequently, we utilized MEGA11 to conduct a phylogenetic tree analysis between the OmpH of other species and these five proteins using the neighbor-joining method.

Construction of the *OmpH* Mutant Strain

The *OmpH* knockout strain was constructed using CRISPR-Cas9 gene editing system following the procedure described by Wang et al.[28] The pCasAb and pSGAb plasmids (provided by Prof. Quanjiang Ji, Shanghai University of Science and Technology) were *A. baumannii* shuttle plasmids expressing Cas enzyme, RecAb recombinase, and sgRNA. Single-stranded DNA (ssDNA) from the homologous repair arm was synthesized by Sangon Biotech Co. Ltd. (Shanghai Co., China). *A. baumannii* receptive cells were obtained by washing with precooled 10% sterile glycerol at 4°C. pCasAb, pSGAb, and single-stranded DNA (ssDNA for homologous repair) were electroporated successively. After pCasAb electrotransformation, RecAb recombinase and Cas9 nuclease expression were induced with isopropyl-beta -D-thiogalactopyranoside (IPTG). Positive transformants were screened using corresponding plasmid resistance gene fragments. Colony PCR was performed to verify the *OmpH* mutation and sequencing was performed to verify the accuracy of the results.

ΔOmpH Complementation Strain Construction

The *OmpH* gene was amplified using the following cloning primers [*OmpH*-F (5′→3′), CGCGGATCCT GGTCCAATTTGGTACAGAG; *OmpH*-R (5′→3′), GCTCGAGTGCGGCCGCACTCGCCAAGTTTGAAAATT]. It was attached to *Bam*HI and *Not*I sites of the pYMAb2-Hyg plasmid. The *A. baumannii* shuttle plasmid was provided by Hua Xiaoting. The constructed positive vector was transformed into the corresponding deletion strain by electrotransformation to obtain a complementary strain, Δ*OmpH*, and electroporated empty vector pYMAb2-Hyg plasmid to Δ*OmpH* as vector control. The accuracy of complementation was verified by sequencing.

Determination of Growth Curve

The concentration of the fresh bacterial solution was adjusted to 1×10^6 CFU/mL using a TSB liquid medium, and 200 μL bacterial solution were added to each well of a 96-well plate, which was incubated continuously for 24 h. The optical density (OD) was determined using the Multifunction Enzyme Labeler Agilent BioTek Cytation5 every 2 h to measure the bacterial concentration.

Quantification of Biofilm Formation in *A. Baumannii*

The yield of *A. baumannii* biofilms was quantified using crystal violet staining as previously method.[29] After the removal of the bacterial solution, the cells were washed and resuspended. The concentration was adjusted to 1×10^6 CFU/mL using TSB liquid medium. Next, 200 μL of the bacterial solution was added to each well of a 96-well plate with three replicates per group. The control group received an equal volume of TSB liquid medium. The plates were incubated at 37 °C for 24 h. The free bacteria were removed and 200 μL of 10% methanol per well was added after washing with sterile PBS. The biofilm was fixed for 30 min, stained with 0.1% crystal violet solution, and the OD_{620} was measured by dissolving crystal violet in 95% ethanol after washing three times with PBS.

Gene Expression Analysis

Total RNA was isolated using an RNA extraction kit M5 EASY spin plus (Mei5 Biotechnology Co. Ltd). Complementary DNA (cDNA) was reverse transcribed using a reverse transcription kit RR047A (Takara). RT-qPCR was performed in 10 μL reactions, with ROX and 16S ribosomal RNA (rRNA) as internal controls (Table S1). The expression of genes with the greatest transcriptome difference (*H1126, H1233, H3691, CspG, GspG*, and *PaaH*) and

biofilm-related genes were determined before and after *OmpH* knockdown using the $2^{-\Delta\Delta CT}$ method. The detailed sequences for target genes and biofilm-associated genes were presented in Tables S2 and S3.

MIC (Minimal Inhibitory Concentration) Assay Before and After Gene Knockdown

Following a previously published method,[30] 100 μL of Mueller-Hinton Broth (MHB) liquid medium was added to each well of a 96-well plate. Then, 128 μg/mL of Cec4 solution was added to the final well. Take 100 μL per well and dilute it sequentially. The final concentrations of 100 μL of the medium in each well were 2, 4, 8, 16, 32, and 64 μg/mL. The negative control and blank control groups did not receive the Cec4 solution. Then, a bacterial solution with a concentration of 2×10^6 CFU/mL was added to each well, except for the blank control, and the final concentrations of Cec4 after addition were 1, 2, 4, 8, 16, and 32 μg/mL. Three replicates were used for each treatment. The 96-well plates were incubated at 37°C for 16–20 h. According to the Clinical and Laboratory Standards Institute (CLSI) standards, MIC is defined as the lowest concentration of a drug that visibly inhibits bacterial growth.

Broth and Agar Dilution Methods

Based on a previously published method with slight modifications,[30] 1/2 MIC of Cec4 was added to LB solid medium and different concentrations of the bacterial solution (1–10^6 CFU/mL) were spotted onto resistant plates. The growth of colonies was analyzed after 8 h.

MBC Assay

TSB liquid medium with sequential additions of Cec4 at final concentrations of 1/16×MIC, 1/8×MIC, 1/4×MIC, 1/2×MIC, 1×MIC, 2×MIC, 4×MIC, and 8×MIC were used. Three replicate wells were used for each concentration and the culture was maintained at a constant temperature of 37°C. The blank control group received 200 μL of TSB liquid medium and the negative control group received only the bacterial solution. The final bacterial concentration in the TSB liquid medium was adjusted to 1×10^7 CFU/mL according to a published method.[31] As mentioned above, the inhibition of Cec4 on the biofilm formation by *A. baumannii* before and after gene knockout was determined by crystal violet staining.

MBEC Assay

The bacterial solution was prepared in a TSB liquid medium at a concentration of 1×10^6 CFU/mL. Then, 200 μL of the solution was inoculated into each well of a 96-well plate as published method.[32] TSB liquid medium without bacterial solution was used as a blank control. The plate was incubated at a constant temperature of 37°C for 24 h. The TSB liquid medium was prepared with final concentrations of 4, 8, 16, 32, 64, 128, 256, and 512 μg/mL Cec4. The culture supernatant was then replaced with the prepared medium. The negative control group received TSB liquid medium without Cec4. Each treatment was performed in triplicates. The plates were incubated at 37°C for 24 h. The biological periplasm content in the wells was quantified using crystal violet staining. The clearance rate was calculated according to the following formula: clearance rate = (1 × experimental group OD_{620}/control group OD_{620}) × 100%. The $MBEC_{50}$ values for each group were calculated and recorded.

The Capsule Staining Experiment

The slide was dripped with 10 μL of Congo red dye and 3 μL of bacterial solution (1×10^6 CFU/mL). When the solution on the slide was air-dried, 5% diluted hydrochloric acid was added for 30 s for decolorization. The slides were then rinsed with ddH_2O. An equal volume of crystal violet staining solution was dripped onto the slide, left for 1 min, and rinsed with ddH_2O. After drying, the slides were placed under a 100× inverted microscope (CKX53; OLYMPUS) and photographed.

Statistical Analysis

Bioinformatic-related images and graphs were generated using R v4.2.1. Other images and graphs were generated using GraphPad Prism 9. A *t*-test was used to compare two groups, and a one-way analysis of variance (ANOVA) was used to compare more than two groups.

Results

Transcriptome of *A. Baumannii* with Strong Biofilm Phenotype After Cec4 Treatment

As our previous study did not thoroughly investigate the mechanism by which Cec4 removes biofilm, we obtained transcriptome data of *A. baumannii* with a strong biofilm phenotype after Cec4 treatment in the previous study and re-matched it to the ATCC19606 genome for reanalysis. The results showed that the direct downstream sequencing data contained a certain number of adapter-containing reads as well as low-quality, N-containing reads, and the quality control process then filtered the above reads (Tables S4 and S5). And a portion of poor-quality fragments would be discarded after the quality control, and taking the single-end sequencing results of ABF1 as an example, the quality control results obtained by the fastp software are shown in Figure S1, which shows that the quality of illumina sequencing platform is better, the quality of base sequencing is slightly improved after filtering, and the overall difference is not significant (Figure S2).

After comparing the quantitative results (Figure S3), we also found by PCA analysis (Figure S4) that although there were outliers in the between-sample group differences for the Con2 and ABF4 samples, the overall distribution showed that the between-sample group differences were greater than the within-group differences because of the downscaling of the between-sample differences by PCA analysis. Therefore, we concluded that the gene expression of the samples in the present study was in accordance with the requirements of the subsequent analyses.

Based on the above results, we performed a difference analysis using the coefficient of variation matrix after normalizing the gene expression results (counts) before and after Cec4 treatment, and the final results showed that the transcriptome of Cec4-treated *A. baumannii*. compared to that of the untreated group of *A. baumannii*. We identified 425 differentially expressed genes, with 242 upregulated and 183 downregulated genes, using $|\log_2\text{Fold Change}|$ ($|\log_2\text{FC}|$) > 1 and $P < 0.05$. We generated a volcano plot to display these results (Figure 1A), with annotated points representing genes that met the criteria. We selected the top 20 genes based on $|\log_2\text{FC}|$ to generate a heatmap of gene expression and observe the consistency of expression within the group. The color in Figure 1B indicates the gene expression after normalization. The genes showed consistent expression within the group, and those with significant differences after Cec4 treatment were mostly upregulated.

Gene Ontology (GO) enrichment analysis of the differentially expressed genes revealed significant enrichment in four pathways: secondary metabolic processes, redox processes, monocarboxylic acid catabolism, and oxidoreductase activity (Figure 1C). The Kyoto Encyclopedia of Genes and Genomes (KEGG) pathway enrichment analysis of the differentially expressed genes showed significant enrichment in three pathways: sulfur metabolism, ABC transport, and the two-component system (Figure 1D).

RT-qPCR Validates the Transcriptome

To assess the accuracy of the transcriptomic analysis, we selected some of the genes that we quantified based on transcriptomics as well as genes with significant differences based on transcriptomics for reverse transcription quantitative polymerase chain reaction (RT-qPCR) validation. We found that *HMPREF0010_02297*(*H2297), PgaA, HMPREF0010_02766* (*H2766), HMPREF0010_01126* (*H1126), GspG, HMPREF0010_02313* (H2313), *HMPREF0010_03691* (H3691), *PaaH CspG* and *HMPREF0010_01233* (H1233) were upregulated or downregulated in a manner consistent with the transcriptomic analysis (Figure S5).

Analysis of Key Genes During Cec4 Clearance of *A. Baumannii* Biofilms

In the process of finalizing the knockout genes in the transcriptome, the thresholds for differential genes were adjusted to further narrow down the range, adopting *padj* < 0.05 as the significance threshold, and 338 differential genes were obtained after the adjustment, with 208 upregulated genes and 130 downregulated genes (Figure 2A). Sixteen genes were involved in the ABC transporter pathway (Figure 2B), and these genes were functionally related to the inner membrane components of the binding protein-dependent transport system, transport of amino acids, and sulfur/phosphate transport. The genes enriched in this pathway were mainly Glt-family and Ssu-family genes, with Glt-family genes generally showing downregulation and Ssu-family genes generally showing upregulation. In addition, antimicrobial peptides

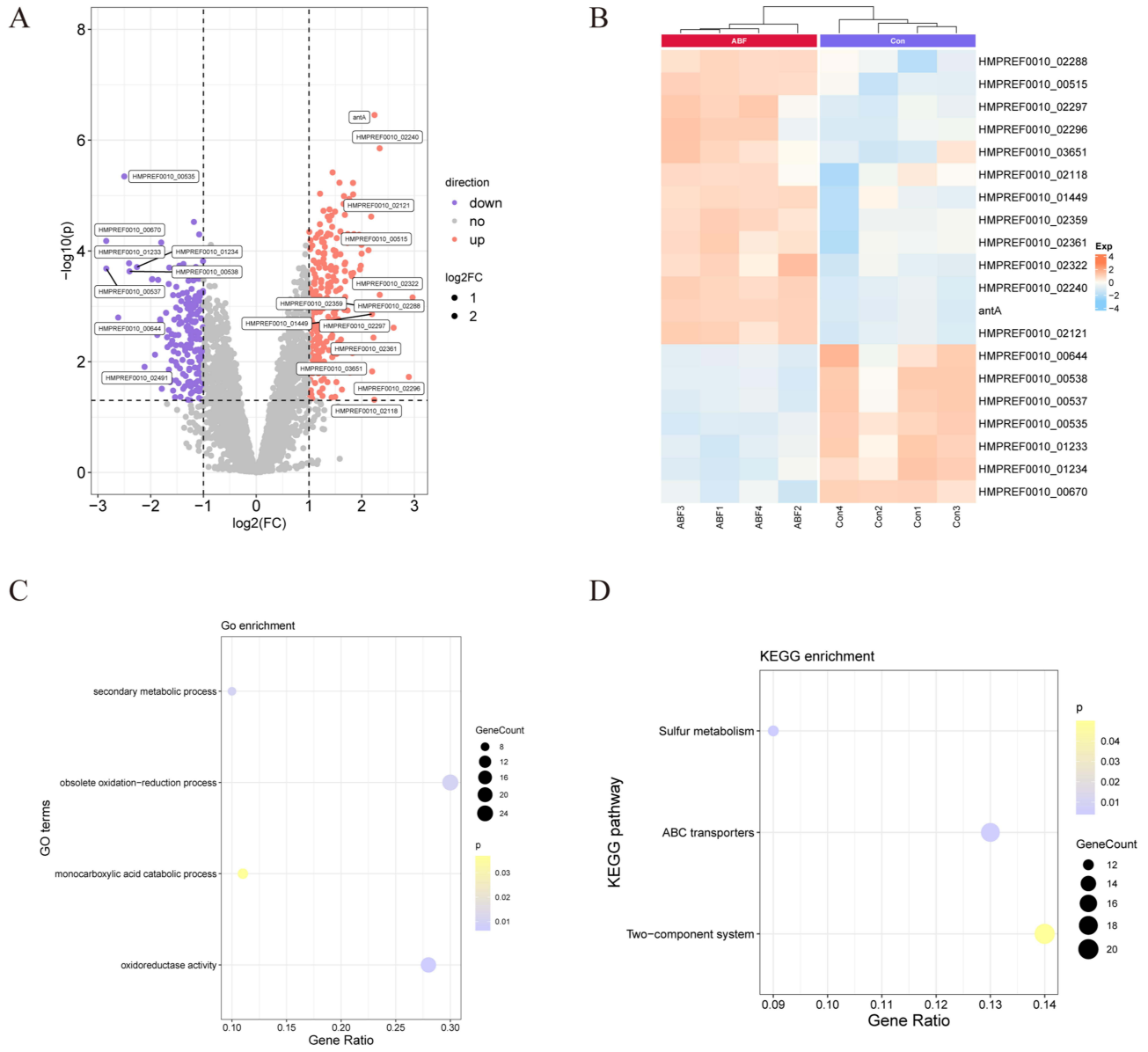

Figure 1 Transcriptomic analysis of *A. baumannii* with strong biofilm treated by Cec4. (**A**) The differential gene volcano map. Genes with $|\log_2 FC| > 2$ and $P < 0.05$ are annotated in the volcano plot. (**B**) The heat map of the expression of the top 20 differential genes. The figure displays gene expression after normalization, with colors indicating the levels. The results indicate that most genes exhibit consistent intragroup expression, while genes with significant differences after Cec4 treatment show up-regulation. (**C**) The bubble map of differential gene GO enrichment. (**D**) The bubble map of differential gene KEGG enrichment.

inhibit or scavenge the biofilm process, possibly by interfering with cell signaling, inhibiting bacterial response processes, downregulating binding protein transporter genes responsible for biofilm formation, and interfering with the bacterial membrane potential in the biofilm, thereby disrupting the biofilm. Differential genes were analyzed for functional enrichment to select significantly enriched pathways as described previously. GO was enriched for redox process (BP) and oxidoreductase activity (MF), and KEGG was enriched for ABC transport (Figure 3A and B). GO enrichment analysis involved a total of 22 related genes after narrowing down the scope, all of which were related to redox processes, but in this study, the probability of proteins involved in the redox process of bacterial cells to be the key genes of Cec4 affecting the biofilms of *A. baumannii* was small, and the redox-related proteins were involved in a wider range of proteins, therefore, the related genes were not selected as candidate genes from GO-enriched pathways. However, the GO enrichment results further illustrated the interference of Cec4 with redox processes in *A. baumannii*. Therefore, according to the above process, the ABC transporter-related pathway proteins in the KEGG pathway were

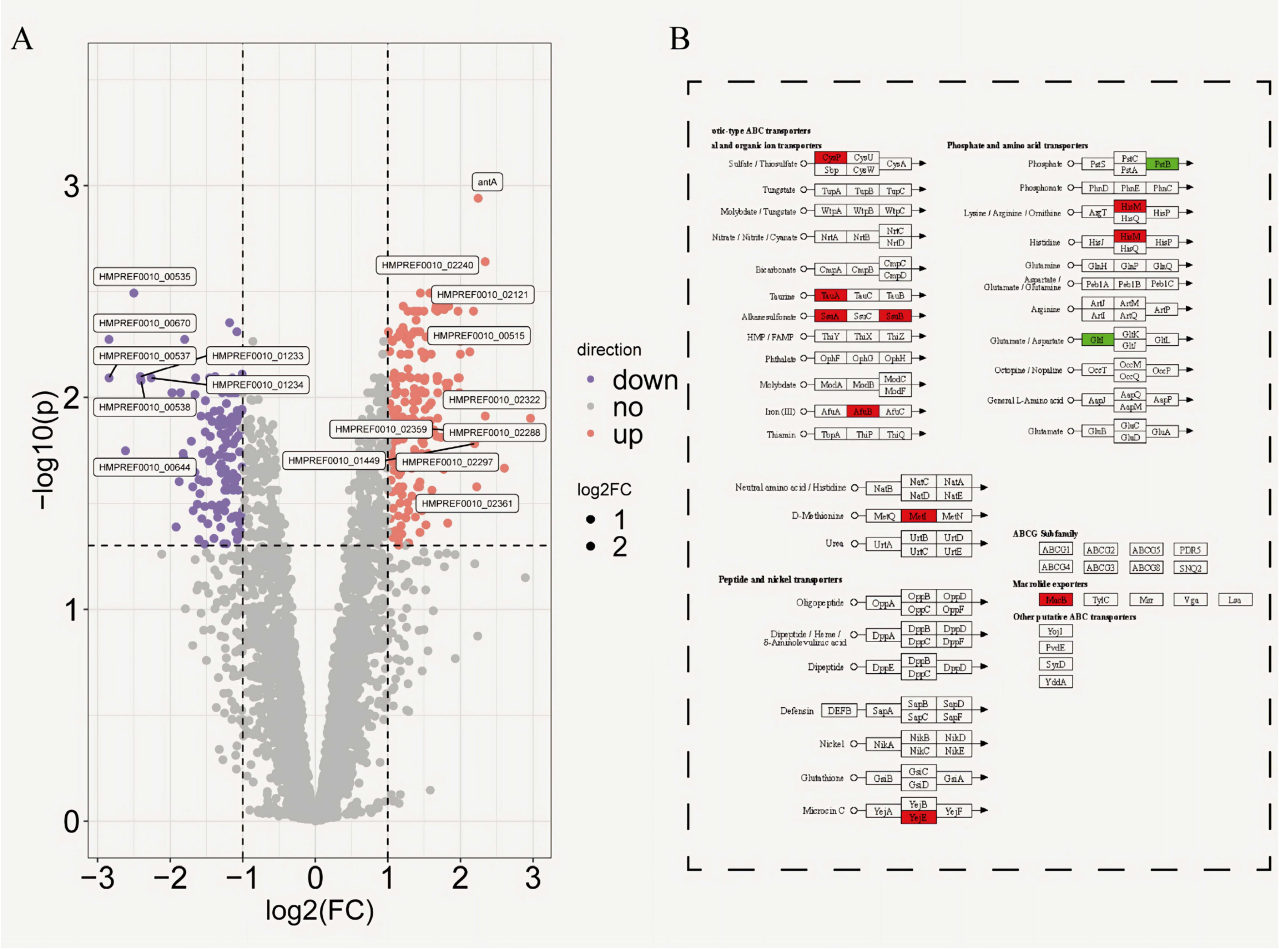

Figure 2 Adjusted differential genes and differential genes in the ABC transport pathway. (**A**) The padj differential gene volcano map. (**B**) The gene enriched in the ABC transporter pathway obtained after KEGG functional enrichment of the differential gene in A.

selected, and the outer membrane-related proteins were selected as candidate genes based on differential gene annotation, and the detailed candidate genes are shown in Table 1.

Based on our previous findings, Cec4 and *A. baumannii* co-localization laser confocal results indicated that Cec4 was located on the outer membrane of *A. baumannii*. Therefore, we focused on seven genes in the transcriptome that were associated with the outer membrane (Table 1). Only three genes were downregulated and *HMPREF0010_00354* (*OmpH*) was downregulated and had a corresponding protein. Thus, we selected *OmpH* which has not been previously explored in *A. baumannii*. Structural domain prediction confirmed that the protein's structural domain was OmpH (Figure 4A). At the same time, the results of *OmpH* knockout were shown (Figure 4B). Bioinformatic prediction suggested that this gene consists of 167 amino acids and may undergo N-terminal cleavage of a 23-residue signal peptide. The anterior and posterior halves of the protein exhibited hydrophobicity and hydrophilicity, respectively. The molecular weight of the protein is 18710.3 Da, and a transmembrane region is predicted (Figure S6), which is consistent with the *OmpH*-like proteins found in *Xanthomonas caldophilus*. We predicted the three-dimensional structures of OmpH and Cec4 (Figure 4C and D) and performed protein-to-protein docking of OmpH and Cec4 using DS2019 (Figure 4E). In addition, a phylogenetic tree was constructed for this gene (Figure 4F). The results showed that *OmpH* homology between *A. baumannii* and other species was not high.

OmpH Gene Knockout

We constructed *OmpH* deletion strains using the CRISPR-Cas9 gene-editing system (Figure S7A–D). Subsequently, we constructed a vector plasmid containing the entire *OmpH* gene fragment, using the expression plasmid pYMAb2-Hyg for

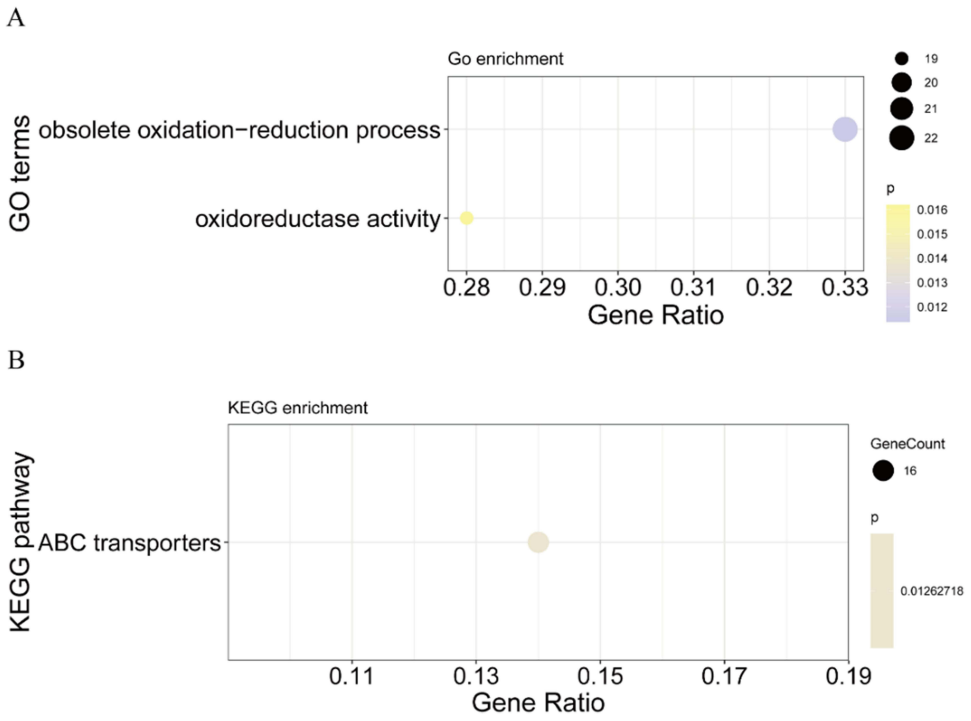

Figure 3 Bubble plots of GO and KEGG enrichment . (**A**) The adjusted GO significantly enriched pathway. (**B**) The adjusted KEGG significantly enriched pathway.

complementation (Figure S7E and F). Furthermore, the pSGAb plasmid in the CRISPR-Cas9 system carries a kanamycin-resistance tag. However, clinical strain CRAB78 is resistant to this antibiotic; therefore, we chose ATCC 17978 to construct the deletion strain.

Effects of *OmpH* Gene on *A. Baumannii* Growth and Biofilm Formation

We investigated the growth (Figure 5A) and biofilm formation (Figure 5B) of the wild-type (ATCC 17978), *OmpH*-knockout (*ΔOmpH)*, and back-complemented (*ΔOmpH::OmpH)* (Figure S8A). The growth curves of ATCC 17978, *ΔOmpH*, and *ΔOmpH::OmpH* were almost identical up to 4h of incubation. *ΔOmpH* growth was slightly lower than that of ATCC 17978 and *ΔOmpH::OmpH* from 4 to 8 h. However, after 10 h, the growth curves of the three strains completely overlapped (Figure 5A). This result indicates that *OmpH* gene deletion did not significantly affect the overall growth of *A. baumannii*. In addition, we found that *ΔOmpH* produced significantly more biofilm than ATCC 17978 ($P < 0.05$), and a similar amount of biofilm as the *ΔOmpH::OmpH* strain (Figure 5B). Previous studies have demonstrated that the *OmpH* gene serves as the upstream regulator of *LuxR*. Relevant experiments in *Vibrio alginolyticus*[33] indicated that the regulation of *OmpH* on the *LuxR* gene and biofilm was influenced by temperature. At 22°C, the deletion of the *OmpH* gene in *V. alginolyticus* resulted in the up-regulation of the *LuxR* gene and a significant reduction in biofilm formation. Nevertheless, at 37°C, the *OmpH* deficient strain exhibited significantly higher biofilm production than wild strains. In this study, the culture condition for *A. baumannii* was 37°C, and we ventured a bold speculation that the reason for the increase in biofilm formation might be associated with temperature.

Effect of *OmpH* Gene Deletion on *A. Baumannii* Sensitivity to Cec4

We evaluated the sensitivity of *A. baumannii* to Cec4 after the *OmpH* gene be knocked out. The MIC of *ΔOmpH* was approximately one gradient lower than that of ATCC 17978 (Figure S8B), approximately 2–4 μg/mL, and the MIC of ATCC 17978 was approximately 4 μg/mL. Regarding the sensitivity of the wild-type and *OmpH* deletion strains to Cec4, we also conducted agar spot plate experiments, and the results were consistent with the MIC results (Figure 5C). This suggests that deletion of *OmpH* makes ATCC 17978 more sensitive to Cec4.

Table 1 The Candidate Genes Selected from the Transcriptome

Gene	Protein	log_2FC	*P* value
KEGG-ABC transporter			
aotQ	–	1.479873143	0.000332958
glnQ	D0C804	−1.658356275	0.000395028
gltI	D0C807	−1.603455392	0.009493657
gltK	D0C805	−1.45762851	0.000184436
hisM	–	1.29203391	0.000113647
HMPREF0010_00886	–	1.189703016	0.001059408
HMPREF0010_01038	–	1.290063642	0.000108447
HMPREF0010_01713	–	1.153820896	0.003645927
HMPREF0010_02504	D0CCM4	1.515294175	0.000346461
HMPREF0010_02965	–	1.034329905	0.001250861
HMPREF0010_03358	–	1.46539906	0.001734293
HMPREF0010_03359	D0CF29	1.033785341	0.006549767
HMPREF0010_03362	–	1.095054779	0.000570843
metI	–	1.44042682	0.003325411
pstB	D0CBX9	−1.516288566	0.001054119
tauA	D0C855	1.105759376	0.007925973
Anno-Outer membrane			
HMPREF0010_00354	D0C6H4	−1.173563632	0.000844949
HMPREF0010_00477	D0C6U7	1.494831376	1.95E-05
HMPREF0010_00883	D0C803	1.675727823	0.000174084
HMPREF0010_01445	–	1.210494913	0.001251835
HMPREF0010_01710	–	−1.315163688	0.00056472
HMPREF0010_01714	D0CAD4	1.14440349	0.000746119
oprM	D0CDQ0	−1.061593702	0.003945246

Notes: "–" in the table indicates genes that do not correspond to proteins in the transcriptome; KEGG-ABC transporter is ABC transporter-related genes in the KEGG significantly enriched pathway; and Anno-Outer membrane is genes related to the outer membrane in the differential gene annotation.

The Cec4 MBC of strain *ΔOmpH* was the same as that of strain ATCC 17978 (both 8 μg/mL); although the biofilm of *ΔOmpH* was slightly higher than that of ATCC 17978 at 1, 2, and 16 μg/mL, but the difference between strains was not significant (Figure 5D).

The $MBEC_{50}$ measurement showed that the $MBEC_{50}$ of Cec4 for *ΔOmpH* was 256 μg/mL, while the $MBEC_{50}$ of ATCC 17978 did not fully reach 50% removal efficiency at 512 μg/mL, and the removal efficiency of *ΔOmpH::OmpH* reached 50% at 512 μg/mL. Therefore, the results showed that the Cec4 clearance efficiency of *ΔOmpH* biofilm was slightly but significantly higher than that of the ATCC 17978 biofilm ($P < 0.05$) (Figure 5E). In summary, it is possible that *OmpH* interacts with Cec4 during the Cec4-mediated removal of *A. baumannii* biofilms.

Effect of *OmpH* Gene on Capsule Thickness of *A. Baumannii*

Capsules play an important role in *A. baumannii* biofilm formation. We stained the capsules of strains *ΔOmpH* and ATCC 17978. The extracellular region is colored pink, the cells are colored purple, and the extracellular transparent circle is the capsule layer. After staining, it is found that the capsular thickness of *OmpH* was significantly reduced (Figure S8C), indicating that *OmpH* could affect or positively regulate the capsule of *A. baumannii.*

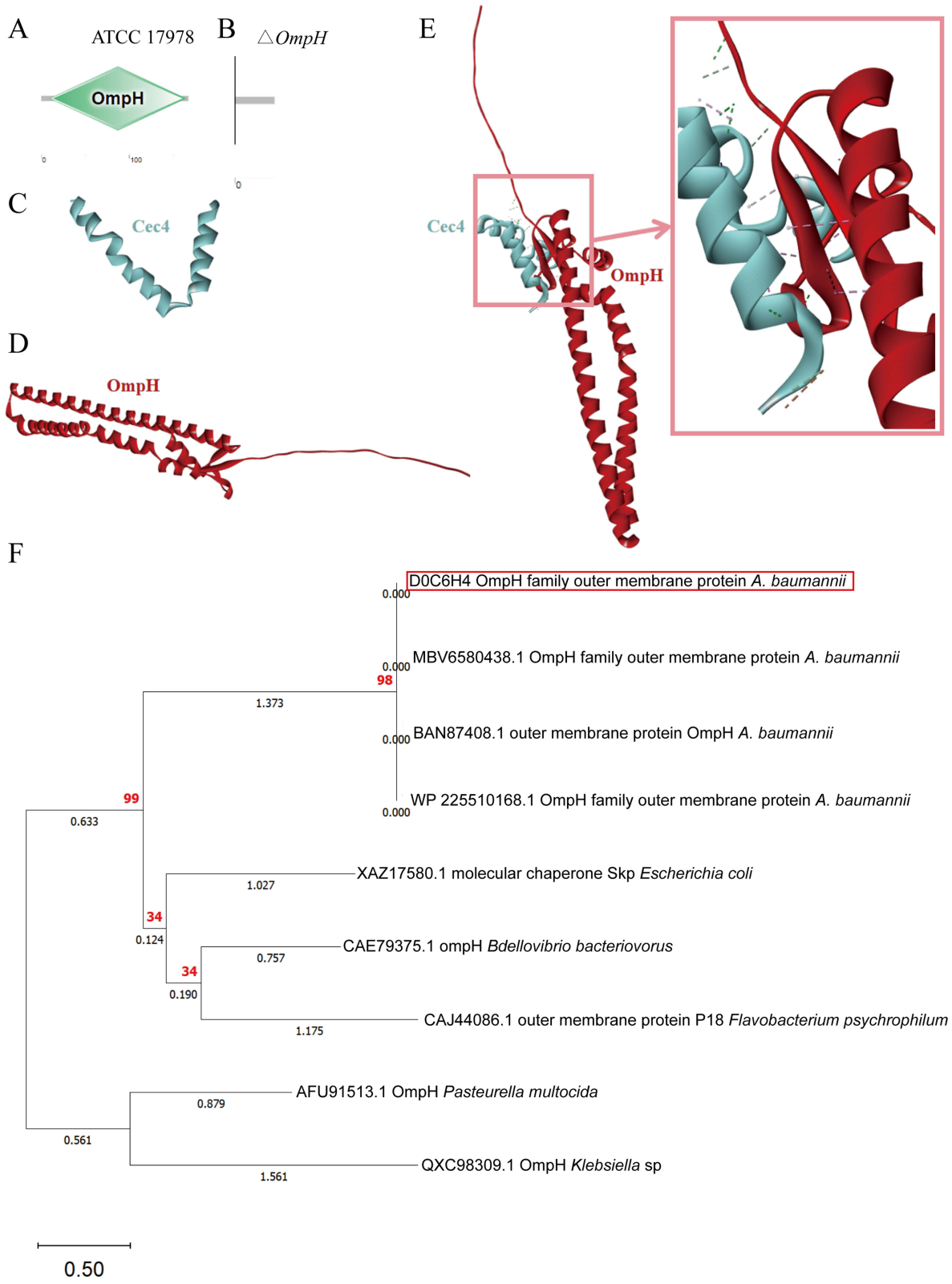

Figure 4 Bioinformatics prediction and molecular docking results for OmpH. (**A**) The SMART-predicted structural domain region of OmpH. (**B**) The SMART-predicted structural domain region of the deletion of the OmpH. (**C**) The 3D protein structure of Cec4 predicted by AlphaFold2. (**D**) The 3D protein structure of OmpH predicted by AlphaFold2. (**E**) The result of protein-to-protein docking for Cec4 and OmpH. (**F**) Results of phylogenetic tree analysis were performed after blast of OmpH. Figure in the red box line is OmpH.

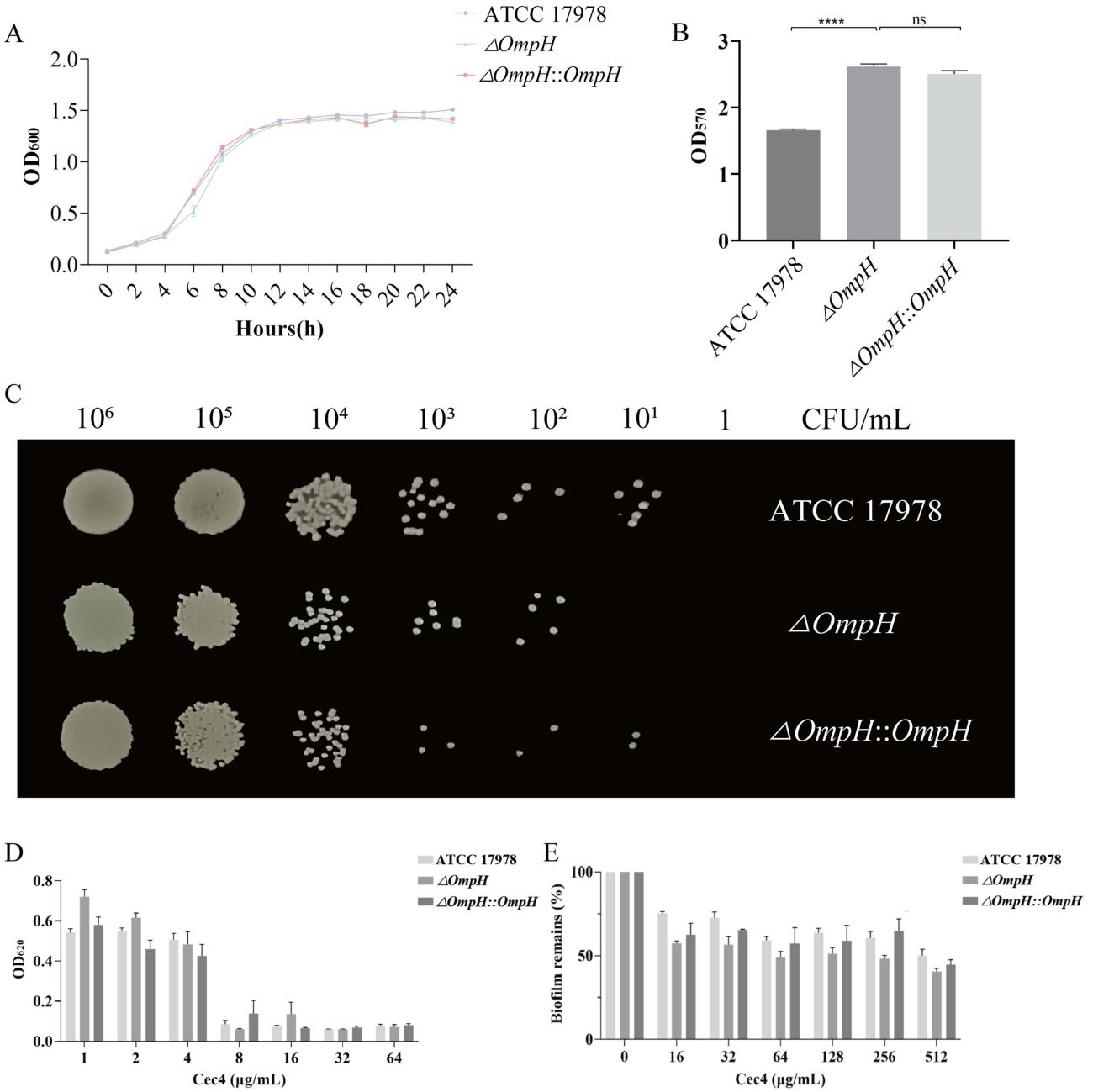

Figure 5 Effect of gene *OmpH* deletion on growth, biofilm formation, and Cec4 sensitivity. (**A**) The growth curves of wild bacteria (ATCC 17978), *OmpH* knockout bacteria (*ΔOmpH*), and back-complemented bacteria (*ΔOmpH::OmpH*). (**B**) The effect of biofilm formation on the growth and susceptibility of wild bacteria (ATCC 17978), *OmpH* knockout bacteria (*ΔOmpH*), and back-complemented bacteria (*ΔOmpH::OmpH*). (**C**) The susceptibility of the *OmpH* deletion strains to Cec4 as tested by an agar spot plate. (**D**) The detection of the OD_{620} MBC results. (**E**) The $MBEC_{50}$ results of the antimicrobial peptide Cec4 against ATCC 17978, *ΔOmpH*, and *ΔOmpH::OmpH*.

Regulatory Role of *OmpH* in *A. Baumannii*

The relative expression level of genes related to biofilm formation before and after *OmpH* gene knockout was verified. The results showed that *BfmR* was upregulated in the two-component system associated with biofilm formation in *ΔOmpH*, while another *BfmS* gene in the two-component system, *CsuE* in the pili system, and phosphoglucose-mutase *PGM* were down-regulated (Figure S8D). Previous studies have shown that the *BfmS* gene is negatively regulated as a *BfmR* sensor in the two-component system,[34] which is consistent with quantitative results. At the same time, in order to ensure the effectiveness of overexpressed strains, we detected the expression of

OmpH gene in wild strains, knockout strains and overexpressed strains by qPCR, and found that *OmpH* was indeed more highly expressed in overexpressed strains. Combined with the results of the capsule thinning of *ΔOmpH*, it is suggested that the regulatory pathway of *OmpH-BfmR-CsuE/PGM* does affect the physiological activity of *A. baumannii*.

Discussion

A biofilm is a collection of microorganisms enclosed in an extracellular matrix that shields them from unfavorable conditions. It typically comprises extracellular DNA, water-soluble polysaccharides, proteins, and non-water-soluble compounds.[35] The components of the biological periplasmic matrix may vary owing to different growth environments or changes in the external conditions.[36] However, the ratios of components and regulatory pathways related to the matrix remain unclear. We previously discovered that Cec4 can strongly resist biofilm formation by *A. baumannii*, we did not determine the mechanism underlying this resistance.[20,21] Therefore, we used transcriptomics to investigate the key genes involved in Cec4 clearance from *A. baumannii* biofilms.

Transcriptomic analysis revealed significant enrichment in three KEGG pathways: sulfur metabolism, ABC transporter, and two-component system. Genes enriched in the sulfur metabolism pathway were primarily focused on the uptake of extracellular sulfate, taurine, and alkane sulfonate. These compounds may be utilized in the carbon sequestration pathways of prokaryotes. Therefore, Cec4 may affect the carbon sequestration pathway of the bacterial cells during biofilm removal. Furthermore, other genes in this pathway participate in processes, such as sulfide oxidoreductases. Genes related to sulfur metabolism have been suggested to be upregulated during bacterial biofilm formation.[37] In this pathway, only one gene was downregulated and the remaining 11 genes were upregulated. This finding suggests that bacteria upregulate genes related to sulfur metabolism during Cec4-mediated biofilm removal.

KEGG enrichment of the transcriptome resulted in three notable pathways: the sulfur metabolism pathway, the ABC transporter pathway, and the two-component system. Most of the genes enriched in the sulfur metabolism pathway were focused on the uptake of extracellular sulfate, aminoethanesulfonate, and streptansulfonate, which may ultimately be utilized in the carbon sequestration pathway of prokaryotic organisms, Cec4 may affect the carbon sequestration pathway of the bacterial during the removal of the biofilms. In addition, other genes in this pathway are involved in processes, such as sulfide oxidoreductases, and it has been indicated[37] that sulfur metabolism-related genes have been shown to be upregulated in bacterial biofilm formation. While only one gene was downregulated in the enriched pathway, the remaining 11 genes showed an upregulation pattern, suggesting that bacterial cells counteracted the reduction of biofilm by upregulating sulfur metabolism-related genes during Cec4 scavenging of biofilm. In addition, since elemental sulfur is mainly used in the biosynthesis of methionine and cysteine in bacteria, we can speculate that treatment with Cec4 causes the synthesis of methionine and cysteine in bacteria may also be blocked. Another pathway, the two-component system is enriched to four genes involved in the uptake and metabolism of acidic amino acids, and it has been reported in the literature[38] that acidic amino acids, such as aspartic acid and glutamic acid, increase the solubility of many insoluble drugs. The four enriched genes were *glnQ, gltK, HMPREF0010_00886*, and *gltI*, homologs of *AatP/M/Q/J* genes, which were significantly downregulated. The downregulation of these genes may also be a part of the process of bacterial action against Cec4. In addition, the two-component system was enriched with genes homologous to the *LuxI/R* system, *bpsI* and *HMPREF0010_03224*, the former being the *LuxI* family acyl-homoserine lactone synthase *SolI* and the latter being the *LuxR* family group-sensing system transcriptional regulator *SolR*. Both showed a trend of upregulation after Cec4 treatment of mature biofilm of *A. baumannii*, but there is no unanimous conclusion on the relationship between *LuxI, LuxR* and biofilm, and some studies have suggested that the downregulation of both may lead to the reduction of biofilm, while others have suggested that both are negatively correlated with biofilm formation.[39] Therefore, the upregulation of genes related to the two in the present study is not certain that the expression of the change in the amount of Cec4 removal of biofilms, but it can be determined that Cec4 deletion affects the population sensing-related pathway genes. The ABC transporter pathway of KEGG was also enriched after narrowing the screen down with padj for transcriptomic differential genes. There were 16

genes co-enriched before and after range narrowing, and the main genes were related to *Glt* and *Ssu* family genes. The Glt family of genes is mainly associated with aspartic acid transport,[40] and according to existing reports,[41] elevated concentrations of aspartic acid inhibit the formation of bacterial biofilms, reduce bacterial adhesion to the surface of objects, and promote the transition of bacterial to the planktonic state. The downregulation of *Glt* family genes after Cec4 treatment may be due to the role of bacteria in maintaining the biofilm state in the fight against Cec4. The *Ssu* family is mainly associated with the transport of aliphatic sulfonates,[42] and current studies do not point to a clear role of this class of genes in relation to biofilm formation. Interestingly, we found that the efflux pump gene *MacB* was significantly upregulated in the transcriptomes of both Cec4-treated planktonic *A. baumannii* and Cec4-induced drug-resistant bacteria during a previous study, and the gene was also upregulated in Cec4-treated *A. baumannii* during the current Cec4 treatment of the biofilm state. *MacB* is mainly used by bacteria to participate in resistance to macrolide antibiotics,[43] which affects the process of bacterial protein synthesis by influencing the action of bacterial ribosomal proteins, which in turn produces a sterilizing effect.[44] Therefore, we hypothesized that *MacB* gene upregulation after Cec4 treatment might be caused by the entry of Cec4 into bacterial cells, affecting ribosome-related functions.

After transcriptome annotation, there were found to be associated with the outer membrane. The aim of this study was to investigate the key genes and related mechanisms of Cec4 to clarify the biofilm state of *A. baumannii*, while the results of previous studies showed that the co-localization results of Cec4 with *A. baumannii* were on biofilms; the differential genes of the outer membrane were selected among the candidate genes, and also because the *OmpH* gene has been mentioned in many studies to have the potential of antigens as OmpH-like proteins. Therefore, it was selected as the *OmpH* knockout strain. The *OmpH* gene is predicted to encode a structural domain like that of OmpH proteins. In *Escherichia coli*, OmpH proteins function as skp periplasmic chaperones. OmpH-like proteins, on the other hand, are modeled as single chains of skp periplasmic chaperones. *Flavobacterium psychrophilum*[25] contains OmpH-like proteins that are approximately 166 amino acids long and contain a signal peptide at the N-terminus. Therefore, these proteins may serve as vaccine antigens. *OmpH*, which contains 167 amino acids and a 22-residue signal peptide at the N-terminus, has the potential to serve as an antigen. However, the growth of *A. baumannii* was not affected by *OmpH* knockout, and the absence of this gene enhanced *A. baumannii* biofilm production. This suggests that the *OmpH* gene may be one of the negative regulators of biofilm formation. When Cec4 targets to OmpH, it may promote the inhibition of OmpH on biofilm formation, resulting in a decrease in the biofilm of bacteria. Therefore, we reviewed the literature and found that *BfmS, CsuE*, and *Pgm* were negatively correlated with biofilms, whereas *BfmR* was positively correlated with biofilms. As shown by the RT-qPCR results, *OmpH* may function as a positive regulator of *BfmS, CsuE*,[45] and *Pgm* and as a negative regulator of *BfmR*. Its deletion downregulated *BfmS*, leading to upregulation of the *BfmR* gene (Figure S8D). In this pathway, *BfmR* positively regulates the TetR family of transcriptional regulators,[46] leading to the upregulation of TetR transcriptional regulators, which further represses the downregulation of the *Pgm* gene, causing a reduction in capsule thickness and an increase in biofilm production in *OmpH* deletion strains. In contrast, *CsuE* showed a downward trend (Figure S8D), suggesting that *OmpH* is more likely to function as a regulator of Cec4 clearance from biofilms than to be directly involved in biofilm synthesis. In the transcriptome, we found that *CsuE* was downregulated, but the difference was not significant. This suggested that *OmpH* is more likely to act on the biofilm clearance process of Cec4. Regulators act rather than passively downregulating. The MIC and $MBEC_{50}$ of Cec4 decreased in *OmpH* deletion strains, indicating that *OmpH* directly affected the sensitivity of *A. baumannii* to Cec4 and that Cec4 might interact with *OmpH* gene. This agrees with the study by Martinez-Guitian et al, where deletion of the gene *OmpH* caused strain susceptible.[47]

Conclusion

To identify the key genes involved in Cec4-mediated biofilm decrease of *A. baumannii*, we identified the target from the transcriptome as the outer membrane protein *OmpH*. The deletion of *OmpH* did not affect the growth of *A. baumannii*, but led to an increase in the total amount of *A. baumannii* biofilm formation, and subsequently decreases in the MIC and

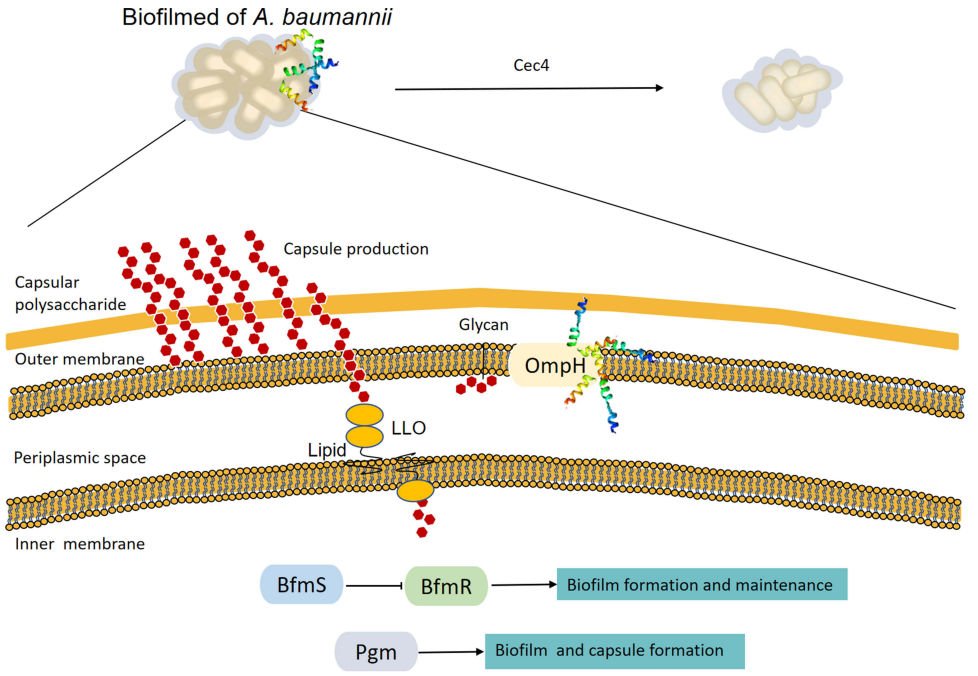

Figure 6 Cec4 decreases the biofilms of *A. baumannii* by *OmpH*. Deletion of the *OmpH* gene affects the two-component *BfmRS* and *Pgm*, which leads to increased biofilms. Finally, it makes the knockout strain more sensitive to Cec4. Glycan synthesis is initiated by a specialized glycosyltransferase, which produces lipo-oligosaccharides (LLO) by transferring sugars to phosphorylated lipids.

$MBEC_{50}$ of *A. baumannii* in response to Cec4. It is hypothesized that *OmpH* may be involved in the removal of biofilm-forming *A. baumannii* as a potential target for the removal of biofilm-forming *A. baumannii* by the antimicrobial peptide Cec4 (Figure 6).

Ethics Approval and Consent to Participate

All materials used in this study were approved by the Institutional Review Board, and all methods and experiments were conducted in accordance with guidelines approved by the Ethics Committee of Guizhou Medical University, China.

Acknowledgments

We would also like to thank Charlotte Brown for proofreading this paper (http://www.proof-reading-service.com). Thanks to Mingyin Xia for his contribution in bacterial biofilm detection and other experiments.

Funding

This research was funded by the National Natural Science Foundation of China (82002180 and 81660347), Guizhou Provincial Natural Science Foundation (ZK [2022] Key Program 039, ZK (2021) Zhongdian 030), China Postdoctoral Science Foundation (2022MD723770), National Foundation Cultivation Project of Guizhou Medical University (21NSFCP39), the undergraduate innovation and entrepreneurship Project (202110660066), the Science and Technology Fund Project of Guizhou Provincial Health Commission (gzwkj2023-567), and the High-Level Talent Initiation Project of Guizhou Medical University (J[2022]023). The funders had no role in the study design, data collection or analysis, preparation of the manuscript, or decision to publish it.

Disclosure

The authors report no conflicts of interest in this work.

References

1. Peleg AY, Seifert H, Paterson DL. Acinetobacter baumannii: emergence of a successful pathogen. *Clin Microbiol Rev*. 2008;21(3):538–582. doi:10.1128/CMR.00058-07
2. Giammanco A, Calà C, Fasciana T, Dowzicky MJ. Global assessment of the activity of tigecycline against multidrug-resistant gram-negative pathogens between 2004 and 2014 as part of the tigecycline evaluation and surveillance trial. *mSphere*. 2017;2(1). doi:10.1128/mSphere.00310-16
3. Theuretzbacher U, Bush K, Harbarth S, et al. Critical analysis of antibacterial agents in clinical development. *Nat Rev Microbiol*. 2020;18(5):286–298. doi:10.1038/s41579-020-0340-0
4. MacNair CR, Brown ED. Outer membrane disruption overcomes intrinsic, acquired, and spontaneous antibiotic resistance. *mBio*. 2020;11(5). doi:10.1128/mBio.01615-20
5. Muhammad MH, Idris AL, Fan X, et al. Beyond risk: bacterial biofilms and their regulating approaches. *Front Microbiol*. 2020;11:928. doi:10.3389/fmicb.2020.00928
6. Upmanyu K, Haq QMR, Singh R. Factors mediating Acinetobacter baumannii biofilm formation: opportunities for developing therapeutics. *Curr Res Microb Sci*. 2022;3:100131. doi:10.1016/j.crmicr.2022.100131
7. Wannigama DL, Hurst C, Pearson L, et al. Simple fluorometric-based assay of antibiotic effectiveness for Acinetobacter baumannii biofilms. *Sci Rep*. 2019;9(1):6300. doi:10.1038/s41598-019-42353-0
8. Shenkutie AM, Zhang J, Yao M, Asrat D, Chow FWN, Leung PHM. Effects of sub-minimum inhibitory concentrations of imipenem and colistin on expression of biofilm-specific antibiotic resistance and virulence genes in Acinetobacter baumannii sequence type 1894. *Int J Mol Sci*. 2022;23(20):12705. doi:10.3390/ijms232012705
9. Lebeaux D, Ghigo JM, Beloin C. Biofilm-related infections: bridging the gap between clinical management and fundamental aspects of recalcitrance toward antibiotics. *Microbiol Mol Biol Rev*. 2014;78(3):510–543. doi:10.1128/MMBR.00013-14
10. Sun F, Qu F, Ling Y, et al. Biofilm-associated infections: antibiotic resistance and novel therapeutic strategies. *Future Microbiol*. 2013;8(7):877–886. doi:10.2217/fmb.13.58
11. Chung PY, Khanum R. Antimicrobial peptides as potential anti-biofilm agents against multidrug-resistant bacteria. *J Microbiol Immunol Infect*. 2017;50(4):405–410. doi:10.1016/j.jmii.2016.12.005
12. Bahar AA, Ren D. Antimicrobial peptides. *Pharmaceuticals*. 2013;6(12):1543–1575. doi:10.3390/ph6121543
13. Saikia K, Sravani YD, Ramakrishnan V, Chaudhary N. Highly potent antimicrobial peptides from N-terminal membrane-binding region of E. coli MreB. *Sci Rep*. 2017;7:42994. doi:10.1038/srep42994
14. Luo Y, Song Y. Mechanism of antimicrobial peptides: antimicrobial, anti-inflammatory and antibiofilm activities. *Int J Mol Sci*. 2021;22(21):11401. doi:10.3390/ijms222111401
15. Overhage J, Campisano A, Bains M, Torfs EC, Rehm BH, Hancock RE. Human host defense peptide LL-37 prevents bacterial biofilm formation. *Infect Immun*. 2008;76(9):4176–4182. doi:10.1128/IAI.00318-08
16. Wolz C, Geiger T, Goerke C. The synthesis and function of the alarmone (p)ppGpp in firmicutes. *Int J Med Microbiol*. 2010;300(2–3):142–147. doi:10.1016/j.ijmm.2009.08.017
17. Di Somma A, Moretta A, Canè C, Cirillo A, Duilio A. Antimicrobial and antibiofilm peptides. *Biomolecules*. 2020;10(4):652. doi:10.3390/biom10040652
18. Naclerio GA, Sintim HO. Multiple ways to kill bacteria via inhibiting novel cell wall or membrane targets. *Future Med Chem*. 2020;12(13):1253–1279. doi:10.4155/fmc-2020-0046
19. Peng J, Long H, Liu W, et al. Antibacterial mechanism of peptide Cec4 against Acinetobacter baumannii. *Infect Drug Resist*. 2019;12:2417–2428. doi:10.2147/IDR.S214057
20. Peng J, Wang Y, Wu Z, et al. Antimicrobial peptide Cec4 eradicates multidrug-resistant Acinetobacter baumannii in vitro and in vivo. *Drug Des Devel Ther*. 2023;17:977–992. doi:10.2147/DDDT.S405579
21. Liu W, Wu Z, Mao C, et al. Antimicrobial peptide Cec4 eradicates the bacteria of clinical carbapenem-resistant Acinetobacter baumannii biofilm. *Front Microbiol*. 2020;11:1532. doi:10.3389/fmicb.2020.01532
22. Jumper J, Evans R, Pritzel A, et al. Highly accurate protein structure prediction with AlphaFold. *Nature*. 2021;596(7873):583–589. doi:10.1038/s41586-021-03819-2
23. Chen N, Jiang D, Liu Y, Zhang Z, Zhou Y, Zhu Z. Preparation of Escherichia coli ghost of anchoring bovine Pasteurella multocida OmpH and its immunoprotective effect. *BMC Vet Res*. 2023;19(1):192. doi:10.1186/s12917-023-03743-9
24. Saier MH, Ma CH, Rodgers L, Tamang DG, Yen MR. Protein secretion and membrane insertion systems in bacteria and eukaryotic organelles. *Adv Appl Microbiol*. 2008;65:141–197. doi:10.1016/j.aam.2008.01.001
25. Dumetz F, Duchaud E, LaPatra SE, et al. A protective immune response is generated in rainbow trout by an OmpH-like surface antigen (P18) of Flavobacterium psychrophilum. *Appl Environ Microbiol*. 2006;72(7):4845–4852. doi:10.1128/AEM.00279-06
26. Jia J, Zhao M, Ma K, et al. The Immunoprotection of OmpH gene deletion mutation of Pasteurella multocida on hemorrhagic sepsis in Qinghai Yak. *Vet Sci*. 2023;10(3):221. doi:10.3390/vetsci10030221
27. Lahesmaa R, Skurnik M, Vaara M, et al. Molecular mimickry between HLA B27 and Yersinia, Salmonella, Shigella and Klebsiella within the same region of HLA alpha 1-helix. *Clin Exp Immunol*. 1991;86(3):399–404. doi:10.1111/j.1365-2249.1991.tb02944.x
28. Wang Y, Wang Z, Chen Y, Hua X, Yu Y, Ji Q. A highly efficient CRISPR-Cas9-based genome engineering platform in Acinetobacter baumannii to understand the H(2)O(2)-sensing mechanism of OxyR. *Cell Chem Biol*. 2019;26(12):1732–1742.e1735. doi:10.1016/j.chembiol.2019.09.003
29. O'Toole GA. Microtiter dish biofilm formation assay. *J Visualized Exp*. 2011;(47). doi:10.3791/2437-v
30. Wiegand I, Hilpert K, Hancock RE. Agar and broth dilution methods to determine the minimal inhibitory concentration (MIC) of antimicrobial substances. *Nat Protoc*. 2008;3(2):163–175. doi:10.1038/nprot.2007.521
31. Pedonese F, Longo E, Torracca B, Najar B, Fratini F, Nuvoloni R. Antimicrobial and anti-biofilm activity of manuka essential oil against Listeria monocytogenes and Staphylococcus aureus of food origin. *Italian J Food Safety*. 2022;11(1):10039. doi:10.4081/ijfs.2022.10039
32. Abouelhassan Y, Yang Q, Yousaf H, et al. Nitroxoline: a broad-spectrum biofilm-eradicating agent against pathogenic bacteria. *Int J Antimicrob Agents*. 2017;49(2):247–251. doi:10.1016/j.ijantimicag.2016.10.017

33. Zhang Y, Wu X, Cai J, et al. Transposon insertion sequencing analysis unveils novel genes involved in luxR expression and quorum sensing regulation in Vibrio alginolyticus. *Microbiol Res*. 2023;267:127243. doi:10.1016/j.micres.2022.127243
34. Krasauskas R, Skerniškytė J, Armalytė J, Sužiedėlienė E. The role of Acinetobacter baumannii response regulator BfmR in pellicle formation and competitiveness via contact-dependent inhibition system. *BMC Microbiol*. 2019;19(1):241. doi:10.1186/s12866-019-1621-5
35. Neu TR, Lawrence JR. In situ characterization of Extracellular Polymeric Substances (EPS) in biofilm systems. In: Wingender J, Neu TR, Flemming H-C, editors. *Microbial Extracellular Polymeric Substances: Characterization, Structure and Function*. Berlin, Heidelberg: Springer Berlin Heidelberg; 1999:21–47. doi: 10.1007/978-3-642-60147-7
36. Flemming HC, van Hullebusch ED, Neu TR, et al. The biofilm matrix: multitasking in a shared space. *Nat Rev Microbiol*. 2023;21(2):70–86. doi:10.1038/s41579-022-00791-0
37. Zhang W, Wu Y, Wu J, Zheng X, Chen Y. Enhanced removal of sulfur-containing organic pollutants from actual wastewater by biofilm reactor: insights of sulfur transformation and bacterial metabolic traits. *Environ Pollut*. 2022;313:120187. doi:10.1016/j.envpol.2022.120187
38. Warraich AA, Mohammed AR, Perrie Y, Hussain M, Gibson H, Rahman A. Evaluation of anti-biofilm activity of acidic amino acids and synergy with ciprofloxacin on Staphylococcus aureus biofilms. *Sci Rep*. 2020;10(1):9021. doi:10.1038/s41598-020-66082-x
39. Li Y, Wang B, Lu F, et al. Synergistic inhibitory effect of polymyxin B in combination with ceftazidime against robust biofilm formed by Acinetobacter baumannii with genetic deficiency in AbaI/AbaR quorum sensing. *Microbiol Spectr*. 2022;10(1):e0176821. doi:10.1128/spectrum.01768-21
40. McIlwain BC, Vandenberg RJ, Ryan RM. Characterization of the inward- and outward-facing substrate binding sites of the prokaryotic aspartate transporter, Glt(Ph). *Biochemistry*. 2016;55(49):6801–6810. doi:10.1021/acs.biochem.6b00795
41. Su X, Cheng X, Wang Y, Luo J. Effect of different D-amino acids on biofilm formation of mixed microorganisms. *Wat Sci Technol*. 2022;85 (1):116–124. doi:10.2166/wst.2021.623
42. Beale J, Lee SY, Iwata S, Beis K. Structure of the aliphatic sulfonate-binding protein SsuA from Escherichia coli. *Acta Crystallogr F*. 2010;66(Pt 4):391–396. doi:10.1107/S1744309110006226
43. Greene NP, Kaplan E, Crow A, Koronakis V. Antibiotic resistance mediated by the MacB ABC transporter family: a structural and functional perspective. *Front Microbiol*. 2018;9:950. doi:10.3389/fmicb.2018.00950
44. Dinos GP. The macrolide antibiotic renaissance. *Br J Pharmacol*. 2017;174(18):2967–2983. doi:10.1111/bph.13936
45. de Breij A, Gaddy J, van der Meer J, et al. CsuA/BABCDE-dependent pili are not involved in the adherence of Acinetobacter baumannii ATCC19606(T) to human airway epithelial cells and their inflammatory response. *Res Microbiol*. 2009;160(3):213–218. doi:10.1016/j.resmic.2009.01.002
46. Fidopiastis PM, Miyamoto CM, Jobling MG, Meighen EA, Ruby EG. LitR, a new transcriptional activator in Vibrio fischeri, regulates luminescence and symbiotic light organ colonization. *Mol Microbiol*. 2002;45(1):131–143. doi:10.1046/j.1365-2958.2002.02996.x
47. Birkle K, Renschler F, Angelov A, et al. An unprecedented tolerance to deletion of the periplasmic chaperones SurA, Skp, and DegP in the nosocomial pathogen Acinetobacter baumannii. *J bacteriol*. 2022;204(10):e0005422. doi:10.1128/jb.00054-22